

# Operation of a 30-cm Ion Thruster with Small-Hole Accelerator Grids

Richard P. Vahrenkamp\*  
Hughes Research Laboratories, Malibu, Calif.

Small-hole accelerator grid ion optical systems have been tested as a possible means of improving 30-cm ion thruster performance. The effects of small-hole grids on the critical aspects of thruster operation, including discharge chamber performance, doubly charged ion concentration, effluent beam characteristics, and plasma properties, have been evaluated. In general, small-hole accelerator grids are beneficial in improving thruster performance while maintaining low double-ion ratios. However, extremely small accelerator aperture diameters tend to degrade beam divergence characteristics. A quantitative discussion of these advantages and disadvantages of small-hole accelerator grids, as well as resulting variations in thruster operation characteristics, is presented.

## Introduction

THE 30-cm mercury ion thruster has been developed over the past ten years to meet a wide range of prime propulsion applications. The current version of this thruster, designated the engineering model (EM) thruster, has undergone comprehensive performance, endurance, and structural testing. Typically, the thruster operates at a thrust level of 0.135 N, with an effective specific impulse of 3000 sec. A more detailed description of the electrical and mechanical specifications of this thruster design has been presented previously.<sup>1-3</sup>

During the course of the performance evaluation of the 30-cm thruster, significant doubly charged ion fractions were measured. Because of this large double-ion density, severe erosion rates of various thruster surfaces have been observed.<sup>4</sup> By using thicker materials with low sputtering yields, catastrophic failure of such components as the baffle and cathode polepiece can be avoided. However, for components such as the screen grid where the material and thickness are specified stringently, the only recourse appears to be minimizing the doubly charged ion content. A reduction in multiply charged ions can be achieved by readjusting certain operating parameters such as discharge voltage or power (electron volts per ion); however, any appreciable reduction in double ionization achieved by this method generally is accompanied by a reduction in total thruster efficiency. However, thruster operation with the use of small-hole accelerator grid (SHAG) optics has proven to be an effective means of reducing double-ion densities while still maintaining thruster efficiency.<sup>5</sup>

This paper will attempt to investigate in more detail the critical aspects of 30-cm thruster operation with the use of SHAG optics systems. The aspects that will be discussed are 1) the optical properties of various small-hole grids, 2) the plasma properties associated with SHAG optics, and 3) performance/double-ion tradeoffs. The EM thruster and optics system is used as the basis for comparison in these tests, and thus all performance will be evaluated with respect to the normal operating points of this thruster.

## Results and Discussion

### Optical Properties of Small-Hole Accelerator Grids

In general, an ion optics assembly that must utilize extremely small accelerator grid apertures is characterized as a

reduced perveance system with significant ion trajectory crossover in the accelerating region. These factors must be weighed against any performance gains or reduction in multiply charged ions which also are characteristic of SHAG optics. As such, the optics analysis is performed with overall thruster performance in mind, realizing that under certain conditions operation with small accelerator apertures may or may not be ideal strictly from the optical quantity point of view.

The determination of minimum accelerator aperture diameter is done by computer trajectory analysis of a single aperture located in the center region of a typical 30-cm dished grid optics system. The computer program used is described in detail in Refs. 6 and 7 and is capable of calculating self-consistent space-charge flows of axial and planar symmetry. The minimum size is defined as that diameter where ions are just starting to intercept the edge of the accelerator aperture. Throughout the analysis, the following parameters are held constant: 1) screen grid aperture diameter  $d_s = 1.91$  mm, 2) screen grid thickness  $t_s = 0.38$  mm, 3) accelerator grid thickness  $t_a = 0.51$  mm, and 4) intergrid spacing  $l_g = 0.64$  mm. The variables, therefore, are 1) ratio of net-to-total voltage  $R$ , 2) total voltage  $V_T$ , and 3) accelerator aperture diameter  $d_a$ . Since single-aperture effects are being considered, the current per hole for a thruster operating at a typical 2.0-A beam current must be evaluated. This has been performed previously<sup>8</sup> with the results shown in Table 1, where a net voltage of 1100 V and an accelerator voltage of  $-400$  V were used to determine the average perveance requirements for each of four constant current density regions. A trajectory analysis for center region apertures can then be done based on these specifications. The results of such an analysis are shown in Fig. 1a. By reducing the accelerator aperture diameter from the EM specification of 1.52 mm to a smaller diameter of 1.22 mm, the trajectories of Fig. 1b can be obtained, nearing the point at which direct interception would occur. The interesting thing to note is that, by utilizing smaller-diameter apertures with the same ratio of net-to-total voltage, the perveance increases from 4.5 nperv (1 nperv =  $10^{-9}$  I/V<sub>T</sub><sup>3/2</sup>) for the EM optics design to 5.2 nperv for the smaller apertures. It is not necessary to readjust the sheath configuration, since the calculated current uniformity remains constant to within  $\pm 5\%$  for both cases. Thus, the EM optics are not operating at maximum perveance, and the optimum means of increasing this value would be to reduce accelerator aperture diameter to the point of direct interception. However, if a further decrease in aperture size is desired, it then becomes necessary to increase total voltage. This relationship is shown in Fig. 2, where the minimum accelerator aperture diameter is plotted as a function of total voltage. Along with the curve for

Presented as Paper 76-1030 at the AIAA International Electric Propulsion Conference, Key Biscayne, Fla., Nov. 14-17, 1976; submitted Jan. 12, 1977; revision received June 10, 1977.

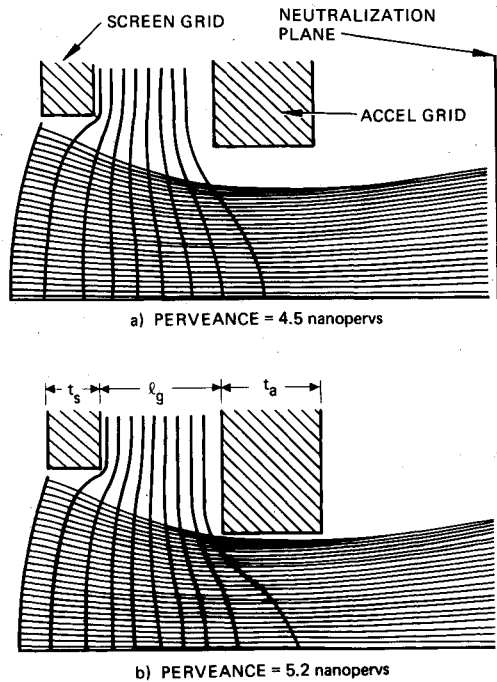
Index category: Electric and Advanced Space Propulsion.

\*Member of the Technical Staff, Ion Physics Department. Member AIAA.

**Table 1** Average current per hole characteristics for 30-cm dished grid at 2-A beam current<sup>a</sup>

Region	Normalized Outer Radius	Number of Holes	Average Current Per Hole, mA	Average Perveance Per Hole, Nanopervs	Total Current, mA
1	0.25	976	0.265	4.56	259
2	0.50	2928	0.220	3.79	644
3	0.75	4880	0.148	2.55	722
4	1.0	6832	0.0548	0.94	374

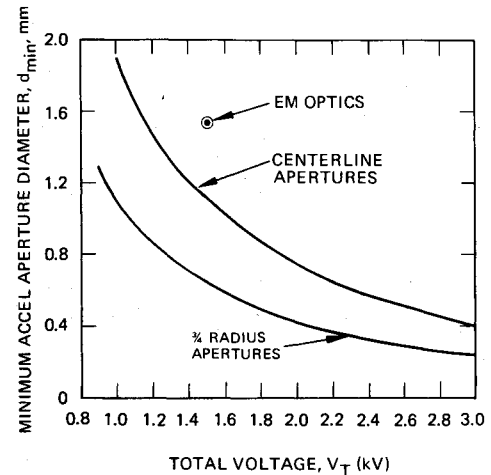
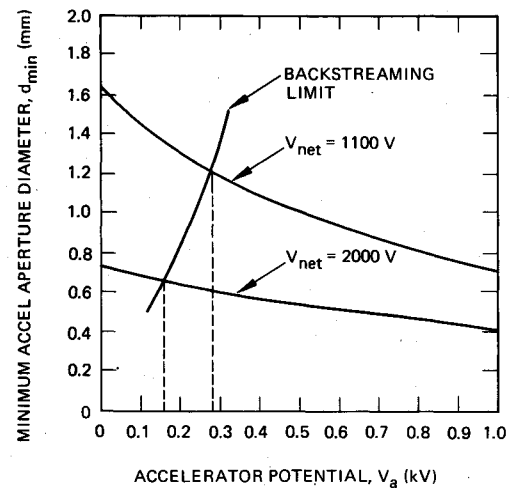
<sup>a</sup> These data were calculated by approximating measured beam profile by four constant current density regions.

**Fig. 1** Effect of reduced accelerator aperture diameter on perveance and trajectories for EM optics ( $V_{\text{net}} = 1100$ ,  $V_a = -400$ ).

center region holes, a curve representative of  $\frac{3}{4}$  radius holes also is shown. These curves are obtained from trajectory plots at continued lower perveance while simultaneously reducing accelerator aperture diameter to the point of direct interception. The ratio of net-to-total voltage is found not to have a significant effect on minimum aperture size; however, it does alter beam divergence characteristics. Knowing the calculated perveance plus the current per hole requirements, it then is possible to determine the total voltage necessary to extract 2.0-A beam current. The maximum theoretical perveance for center region holes is calculated from Child's law for a planar diode. At this point, it is assumed that the accelerator aperture diameter would equal the screen grid aperture diameter. The typical operating point for the EM thruster also is shown in Fig. 2 for reference.

Two parameters that are not reflected in Fig. 2 but that have significant effect on thruster operation are the electron backstreaming limit and the net-to-total voltage ratio. Electron backstreaming occurs when the minimum potential within the accelerator apertures is high enough to permit electrons from the ion beam to flow backwards through the accelerator system. This limit, which is a function of both total voltage and accelerator aperture size, will be discussed first. The accelerator potential  $V_a$  necessary to prevent backstreaming can be estimated by the following relation<sup>9</sup>:

$$V_a = \frac{\exp(t_a/d_a) d_a V_T}{2\pi l_g} \quad (1)$$

**Fig. 2** Theoretical total voltage requirements necessary to avoid accelerator interception on centerline and at  $\frac{3}{4}$  radius ( $l_g = 0.64$  mm,  $d_s = 1.9$  mm,  $I_B = 2.0$  A).**Fig. 3** Backstreaming limits on thruster centerline for optics operating at minimum accelerator aperture diameter.

This relation is plotted in Fig. 3 at the minimum accelerator aperture points, which, in turn specify the total voltage requirements. Also shown are two curves that are replots of Fig. 2, except that the net voltages of 1100 and 2000 V are specified. Thus, at 1100-V net voltage and an accelerator aperture of 1.27 mm diam, approximately -280 V is necessary to prevent both backstreaming and direct interception. At accelerator potentials higher than -280 V, only interception limits aperture size. The curve at 2000-V net voltage demonstrates that SHAG optics would be particularly well suited for high-specific-impulse operation.

The second parameter not reflected in the curves of Fig. 2, and which has significant effect on optical quality, is the ratio of net-to-total voltage  $R$ . Because a 30-cm thruster typically operates at 1100 V, this necessarily dictates low  $R$  values for very-small-hole accelerator grids and, thus, an increase in beam divergence. However, moderate decreases in aperture size to  $\approx 1.1$  mm diam should produce no significant change in trajectories, since a high, nearly constant  $R$  ratio can be maintained, and no change in divergence was noted in the trajectory analysis when the accelerator aperture was decreased to this value.

In order to verify the minimum aperture size analysis, two SHAG ion optics sets were assembled with the specifications listed in Table 2. A screen grid compensation of 0.4% was necessary to correct for the beam divergence loss due to the 2.0-cm dish depth. The EM optics specifications also are

Table 2 Optics specifications

Optics	Screen Aperture Diameter, mm	Accel Aperture Diameter, mm	Grid Spacing, mm	Screen Compensation, %	Dish Depth, cm	Accel Open Area Fraction, %
EM	1.91	1.52	0.63 to 0.68	0.4	2.0	43
SHAG 1	1.91	1.09	0.38 to 0.56	0.4	2.0	23
SHAG 2	1.91	0.69	0.51 to 0.66	0.4	2.0	9

Table 3 Beam dispersion data

Optics	$V_{net}$ , V	$V_a$ , V	FWHM (degrees)		R	$F_T$
			$C_L$	3/4 R		
EM	1100	300	10.0	10.0	0.786	0.983
EM	1100	400	11.0	12.0	0.733	0.982
EM	1100	500	12.0	13.5	0.688	0.981
SHAG 1	1300	400	11.0	11.0	0.765	0.982
SHAG 1	1100	550	14.5	17.0	0.666	0.979
SHAG 1	1100	600	16.0	19.5	0.647	0.977
SHAG 2	1200	500	16.0	22.0	0.710	0.976
SHAG 2	1250	800	25.0	22.0	0.610	0.970

shown for reference. Tests were conducted not only to measure beam divergence angles but also to evaluate thruster performance and double-ion densities. These latter parameters will be evaluated in a later section, and only optical properties will be discussed at this point. A collimated probe<sup>10</sup> is used to measure divergence angles for the three optics sets at various locations on the thruster radius. Because of the small acceptance angle of the probe, the dispersion curves should be representative of an individual aperture. Table 3 lists full-width-half-maximum (FWHM) angles for the three optics sets operated at various accel-decel ratios. These angles are shown for centerline as well as for  $3/4$  radius holes. The overall thrust factor for beam divergence loss, which is obtained by integration over the thruster radius, is shown in the final column. For both sets of SHAG optics, the total voltage necessary to reduce accelerator current to a minimum level was found to be within  $\pm 5\%$  of the value predicted by the trajectory analysis. The beam dispersion angles are degraded, as anticipated, when smaller accelerator apertures are utilized. The data of Table 3 and the curves of Fig. 2 can be used to estimate the total thrust loss due to beam divergence for SHAG optics systems operating at various net voltages. This is shown in Fig. 4, where thrust factor for beam divergence is plotted as a function of minimum accelerator aperture diameter. As can be seen, the beam divergence tends to increase rapidly at very small aperture diameters, particularly at low specific impulse. However, moderate reduction of aperture size to approximately 1.1 mm, as mentioned previously, would be effective in reducing neutral propellant loss by approximately 50% without a significant increase in beam divergence.

It should be mentioned at this point that thicker accelerator grids also may provide an additional reduction of neutral propellant without affecting either beam trajectories or perveance.<sup>11</sup> However, there are several reasons why this approach may not be satisfactory. First, previous investigations<sup>12</sup> have shown no change in performance when the accelerator grid thickness was increased from 0.51 to 0.76 mm. Second, it is extremely difficult to manufacture an accelerator grid thicker than 0.76 mm utilizing present chemical milling techniques. Finally, increasing the grid thickness leads to a larger volume from which charge-exchange can take place.<sup>13</sup> Thus, it appears that further in-

Table 4 Volume-averaged plasma properties for EM and SHAG 1 optics

Optics	EM	EM	EM	SHAG 1	SHAG 1
Beam Current, A	2.0	1.5	1.0	2.0	1.5
Discharge Voltage, V	37.0	37.0	37.0	30.0	30.0
Discharge Current, A	10.0	7.5	5.0	11.7	9.5
Maxwellian Electron Temperature, eV	3.8	3.6	3.3	2.9	3.0
Primary-to-Maxwellian Electron Density Ratio	0.25	0.35	0.50	0.22	0.19
Primary Electron Energy, eV	27.2	25.5	25.4	19.7	19.6
Electron Density, $(\times 10^{-10} \text{ cm}^{-3})$	16.4	9.0	7.5	12.8	8.3
Plasma Potential, V	36.4	33.8	33.1	22	20.5
Corrected Mass Utilization, %	87.5	85.0	80.0	87.0	86.0

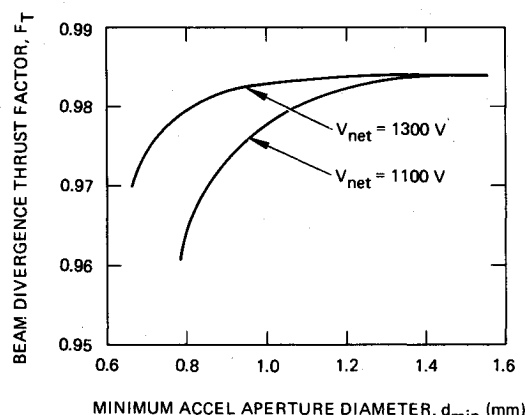


Fig. 4 Beam divergence thrust loss for operation at minimum accelerator aperture diameter.

creasing accelerator grid thickness for a specified aperture size may not be a viable technique for reducing propellant loss.

#### Plasma Properties of SHAG and EM Optics

Because the intent of operating with small-hole accelerator grids is to reduce doubly charged ion densities, a survey of the plasma properties and potential distributions within the discharge chamber was conducted. These properties then can be used as input parameters to double-ion production models,<sup>14</sup> thus indicating the effect that various thruster operating conditions have on double ionization. Because this was the first time a Langmuir probe survey was taken of a 30-cm thruster, EM optics as well as SHAG 1 optics were used in the mappings. The computer technique for analysis of the probe data is described in Ref. 15. The 20 discharge chamber locations used in the mapping procedure were felt to be sufficient to provide an adequate number of points for averaging as well as for distribution plotting. Table 4 summarizes the volume-averaged<sup>14</sup> plasma properties obtained with EM and SHAG 1 optics sets at the operating conditions indicated. The plasma properties and distributions appear to be consistent with those of other ion thrusters for which similar data are available.<sup>16</sup> The main difference between operation with the two optics sets is the lower primary electron energy and lower plasma potential that can be achieved with the use of SHAG optics. This is because stable and efficient operation can be achieved at 30-V discharge

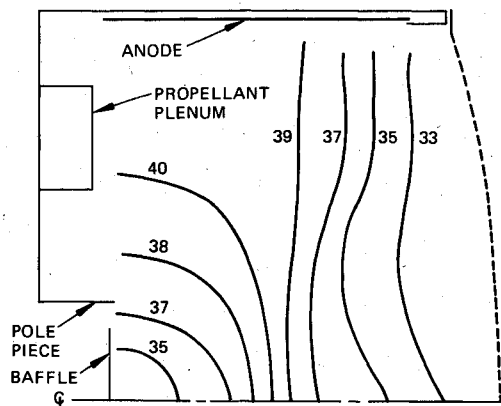


Fig. 5 Schematic of 30-cm thruster showing approximate equipotential lines ( $V_{dis} = 37$  V).

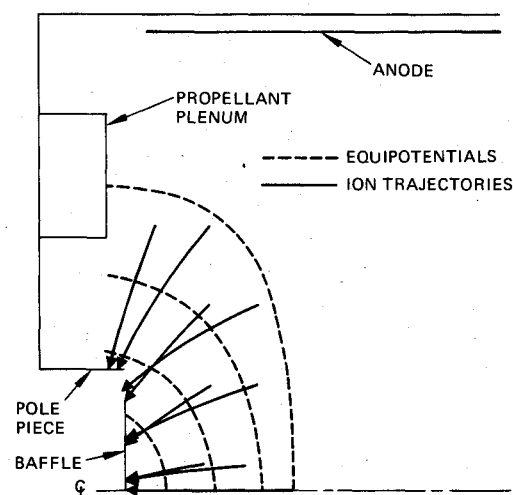


Fig. 6 Simulation of upstream potential distribution showing calculated ion trajectories.

voltage rather than at 37 V. It also should be noted that the primary electron energy of approximately 20 V is within 1.5 V of the threshold energy for double ionization of the single-ion ground state.

It was noted during the probing investigation that a low point in plasma potential existed immediately downstream of the baffle and that the potential appeared to rise by several volts in both the axial and radial directions from this point. This was true for both optics sets and at all operating set points used in the tests. Further analysis was done by constructing approximate equipotential lines throughout the discharge chamber based on the Langmuir probe data. The results are shown in Fig. 5 for EM optics operated at 2.0-A beam current. The shape of the equipotential lines did not change significantly with the substitution of SHAG optics, and such a potential distribution suggests that a significant number of ions formed in the primary electron region never would be extracted by the optics system. Instead, they would be focused toward the baffle and polepiece assembly, causing localized erosion. In order to verify this conjecture, a computer simulation of the potential field was made, and ions were started at arbitrary locations throughout this field. The simulated region of interest is shown in Fig. 6, along with the potential lines and ion trajectories. As can be seen, the ions are, in fact, focused toward the baffle and polepiece, apparently not impinging on the backplate or propellant plenum of the thruster. Since the highest plasma density is on thruster centerline, this suggests a high erosion rate in the center region of the baffle. This modeling seems to be confirmed by the erosion noted in the 10,000-hr lifetest of a 30-cm thruster,<sup>4</sup>

where the center of the baffle was eroded totally after approximately 6000 hr of operation at 1.5-A beam current. This lifetest thruster also showed no erosion of the backplate or the rear half of the cathode polepiece, and thus the model appears to be consistent with experimental results. It is not obvious what changes in the thruster configuration might be made to alter this potential distribution and, thus, reduce the focusing effects. It also was noted in the same lifetest that a significant amount of erosion, not explained by this method, takes place on the upstream surface of the baffle, and further investigation of the cathode region itself appears warranted. It does indicate the need for extremely low double-ion densities if erosion is to be held to an acceptable level.

#### Performance and Double-Ion Production

Knowing the plasma properties of EM and SHAG optics systems, it now is possible to evaluate double-ion production rates for various thruster configurations and operating points. Since small-hole accelerator grids appear to be a possibility for 30-cm thruster operation, the relationships between parameters such as accelerator grid open area fraction, discharge voltage, and mass utilization are reviewed. The following analysis is done, based on a number of simplifying assumptions, to determine the qualitative effect of these parameters on double-ion production. The assumptions that are made include the following:

- 1) Doubly charged ions are generated by electron bombardment of the single-ion ground state.
- 2) The ratio of production rates for single and double ions is a good indication of the double-to-single ion ratio in the beam.
- 3) Only singly charged ions generated from the atomic ground state will be considered.

The first two assumptions introduce very little error into the calculations, and the third is felt to be within the accuracy of the analysis, since approximately 60% of the single ions are produced from the neutral ground state.<sup>14</sup> With these assumptions in mind, the following relationships hold:

$$\dot{n}^{++} = n^+ \left[ \sum_p^+ n_p + \sum_m^+ n_m \right] \quad (2)$$

$$\dot{n}^+ = n_0 \left[ \sum_p^+ n_p + \sum_m^+ n_m \right] - n^+ \left[ \sum_p^+ n_p + \sum_m^+ n_m \right] \quad (3)$$

where  $\dot{n}^{++}$  is the production rate for doubly charged ions,  $\dot{n}^+$  is the production rate for singly charged ions,  $\Sigma_p$  and  $\Sigma_m$  are the electron velocity/cross-section products for primary and Maxwellian electrons,<sup>17</sup> and  $n_0$ ,  $n_p$ , and  $n_m$  are the neutral particle, primary electron, and Maxwellian electron densities, respectively. The following relationships are used to express the densities in terms of current and mass utilization:

$$n_0 = 4I_0 / qv_0 A_a \quad (4)$$

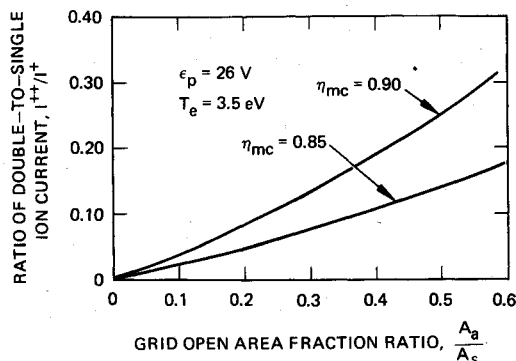


Fig. 7 Effect of grid open area on double-ion content.

$$n^+ = I^+ / qv^+ A_s \quad (5)$$

$$I_0 / I^+ = (1 - \eta_m^+) / \eta_m^+ \quad (6)$$

$$v^+ = \sqrt{(qT_e/m) [1 + (n_p/n_m)]} \quad (7)$$

where  $I_0$  is the equivalent neutral loss current,  $A_a$  and  $A_s$  are the effective open areas of the accelerator and screen grids, respectively, and  $\eta_m^+$  is approximately equal to the corrected mass efficiency  $\eta_{mc}$ . By taking the ratio of Eqs. (2) and (3) and utilizing expressions (4-6), it is possible to arrive at the following relationship for the average double-to-single ion current ratio:

$$\frac{I^{++}}{I^+} \approx 0.707 \times \left\{ \left( \frac{1 - \eta_{mc}}{\eta_{mc}} \right) \left( \frac{v^+}{v_0} \right) \left( \frac{A_s}{A_a} \right) \left[ \frac{\sum_0^+ n_p + \sum_0^+ n_m}{\sum_+^+ n_p + \sum_+^+ n_m} \right] - 1 \right\}^{-1} \quad (8)$$

where  $v^+/v_0$  is the ion-to-neutral-velocity ratio. Thus, the double-ion ratio appears as a function of several other ratios, some of which can be manipulated to achieve a lower double-ion density. Several crossplots of Eq. (8) are made utilizing pertinent data obtained from the Langmuir probe experiments. Figure 7 shows the effect of the accelerator-to-screen open area ratio on the doubly charged ion content in the mass efficiency range of interest. The electron energy  $\epsilon_p$  and temperature  $T_e$  are held constant to average values representative of EM and SHAG optics. Considerable reduction in the doubly charged ion content can be achieved by lowering this ratio, assuming that the mass efficiency can be maintained. Because SHAG optics are a relatively lower perveance system, not only is the accelerator open area lower, but the effective screen area is increased simultaneously because of the increased sheath area. A more comprehensive plot of Eq. (8) is shown in Fig. 8, which includes the effect of discharge voltage. It should be noted that, for low accelerator transmission, the discharge voltage has little effect on the double-ion ratio for a given mass efficiency. It should be remembered, however, that the mass efficiency is also a function of discharge voltage, and, as such, a reduction in discharge voltage will require an increase in discharge current and/or beam current to maintain constant mass utilization efficiency.

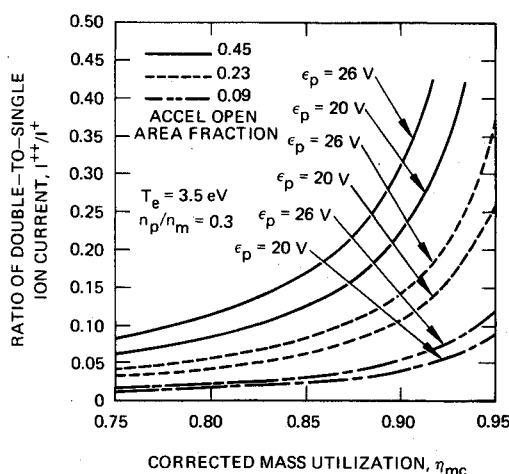


Fig. 8 Theoretical double-ion ratios utilizing parameters representative of EM, SHAG 1, and SHAG 2 optics.

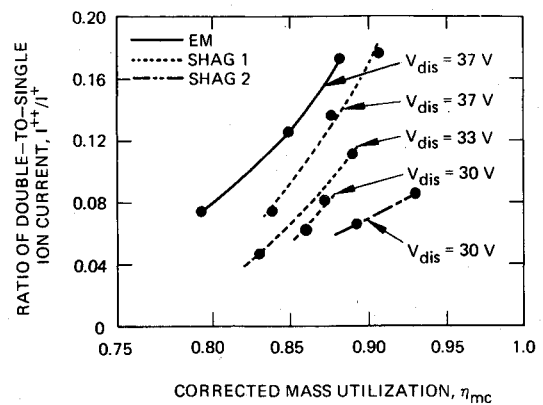


Fig. 9 Double-ion ratios for EM, SHAG 1, and SHAG 2 optics.

Thruster performance was evaluated for the three optics sets listed previously, including double-ion scans utilizing a mass spectrometer probe.<sup>10</sup> The results are shown in Fig. 9, where the data are plotted analogous to Fig. 8. The agreement between the experimental and theoretical curves is good, considering the assumptions that were made. The performance gains that can be realized over EM optics with the use of small accelerator holes are evident with the SHAG 2 optics set. At 2.0-A beam current, a reduction of 50% in doubly charged ions can be achieved while simultaneously increasing the propellant utilization from 88% to 92%.

### Summary and Conclusions

The results of this study can be summarized best by listing the advantages and disadvantages of small-hole accelerator grid ion optical systems for a 30-cm thruster. The principal advantages are as follows:

- 1) Low double-ion ratios can be achieved at thruster design efficiencies.
- 2) Sputtering energy is reduced because efficient operation can be maintained at low plasma potential.
- 3) The increased web thickness allows more area for charge exchange erosion.
- 4) Because of beam size and backstreaming limits, SHAG optics would be well suited for high-specific-impulse operation.
- 5) The larger sheath area of SHAG optics helps reduce screen grid erosion.

The disadvantages are as follows:

- 1) SHAG optics are lower perveance systems if very small apertures are desired.
- 2) At low specific impulse, beam divergence increases significantly for very small apertures.
- 3) A low open area fraction results in more thermal distortion of the accelerator grid.

- 4) At low specific impulse, SHAG optics require higher accelerator potential, thus increasing charge exchange energy.

Thus, there are a number of tradeoffs that must be examined in detail if SHAG optics systems are to be considered for long-term thruster operation. Performance tradeoffs with respect to thruster efficiency and beam divergence can be evaluated readily; however, prime consideration should be given to erosion rates of various thruster components, namely, the screen grid and the accelerator grid. This requires accurate modeling and measurement techniques, and a complete erosion evaluation would be necessary before any long-term testing with SHAG optics could be recommended.

### Acknowledgment

This work was supported in part by NASA Contract NAS 3-19703.

### References

- <sup>1</sup>Poeschel, R.L., King, H.J., and Schnelker, D.E., "An Engineering Model 30 cm Thruster," AIAA Paper 73-1084, Lake Tahoe, Nev., 1973.
- <sup>2</sup>Sovey, J.S. and King, H.J., "Status of 30 cm Mercury Ion Thruster Development," AIAA Paper 74-1117, San Diego, Calif., 1974.
- <sup>3</sup>Collett, C.R., "Endurance Testing of a 30 cm Kaufman Thruster," AIAA Paper 73-1085, Lake Tahoe, Nev., 1973.
- <sup>4</sup>Collett, C.R. and Poeschel, R.L., "A 10,000 Hour Endurance Test of a 700-Series 30-cm Engineering Model Thruster," AIAA Paper 76-1019, Key Biscayne, Fla., Nov. 1976.
- <sup>5</sup>Vahrenkamp, R.P., "An Experimental Investigation of Multiple Ion Processes in Mercury Bombardment Thrusters," AIAA Paper 75-397, New Orleans, La., March 1975.
- <sup>6</sup>Nudd, G.R. and Amboss, K.A., "Effects of Electrode Misalignment and Flow Rate Changes on the Thrust in an Electron Bombardment Engine," *AIAA Journal*, Vol. 8, April 1970, pp. 649-656.
- <sup>7</sup>Hamza, V. and Richley, E.A., "Two-Dimensional Poisson Equation Applied to Electrostatic-Ion-Engine Analysis," NASA TND-1323, 1962.
- <sup>8</sup>Ward, J.W. and Vahrenkamp, R.P., "Characterization of Ion and Neutral Efflux from a 30-cm Mercury Ion Thruster," AIAA Paper 75-357, New Orleans, La., March 1975.
- <sup>9</sup>Kaufman, H.R., "Technology of Electron Bombardment Ion Thrusters," *Advances in Electronics and Electron Physics*, Vol. 36, Academic Press, New York, 1974, p. 301.
- <sup>10</sup>Vahrenkamp, R.P., "Measurement of Doubly Charged Ions in the Beam of a 30-cm Mercury Bombardment Thruster," AIAA Paper 73-1057, Lake Tahoe, Nev., Oct. 1973.
- <sup>11</sup>Aston, G., "The Ion-Optics of a Two Grid Electron-Bombardment Thruster," NASA CR-135034, May 1976.
- <sup>12</sup>Rawlin, V., "Performance of 30-cm Thrusters with Dished Accelerator Grids," AIAA Paper 73-1053, Lake Tahoe, Nev., Oct. 1973.
- <sup>13</sup>Harbour, P.J., "Charge Exchange and Beam Bending at Extraction Electrodes," *Proceedings of the Third European Electric Propulsion Conference*, Hinterzarten, W. Germany, 1974.
- <sup>14</sup>Peters, R.R. and Wilbur, P.J., "A Doubly Charged Ion Model for Ion Thrusters," AIAA Paper 76-1010, Key Biscayne, Fla., Nov. 1976.
- <sup>15</sup>Williamson, W.S., "Discharge-Chamber Sputtering Investigation," AIAA Paper 76-1026, Key Biscayne, Fla., Nov. 1976.
- <sup>16</sup>Masek, T.D., "Plasma Properties and Performance of Mercury Ion Thrusters," *AIAA Journal*, Vol. 9, Feb. 1971, pp. 205-211.
- <sup>17</sup>Ward, J.W. and Masek, T.D., "A Discharge Computer Model for an Electron Bombardment Thruster," AIAA Paper 76-1009, Key Biscayne, Fla., Nov. 1976.

## *From the AIAA Progress in Astronautics and Aeronautics Series...*

### **MATERIALS SCIENCES IN SPACE WITH APPLICATIONS TO SPACE PROCESSING—v. 52**

*Edited by Leo Steg*

The newly acquired ability of man to project scientific instruments into space and to place himself on orbital and lunar spacecraft to spend long periods in extraterrestrial space has brought a vastly enlarged scope to many fields of science and technology. Revolutionary advances have been made as a direct result of our new space technology in astrophysics, ecology, meteorology, communications, resource planning, etc. Another field that may well acquire new dimensions as a result of space technology is that of materials science and materials processing. The environment of space is very much different from that on Earth, a fact that raises the possibility of creating materials with novel properties and perhaps exceptionally valuable uses.

We have had no means for performing trial experiments on Earth that would test the effects of zero gravity for extended durations, of a hard vacuum perhaps one million times harder than the best practical working vacuum attainable on Earth, of a vastly lower level of impurities characteristic of outer space, of sustained extra-atmospheric radiations, and of combinations of these factors. Only now, with large laboratory-style spacecraft, can serious studies be started to explore the challenging field of materials formed in space.

This book is a pioneer collection of papers describing the first efforts in this new and exciting field. They were brought together from several different sources: several meetings held in 1975-76 under the auspices of the American Institute of Aeronautics and Astronautics; an international symposium on space processing of materials held in 1976 by the Committee on Space Research of the International Council of Scientific Unions; and a number of private company reports and specially invited papers. The book is recommended to materials scientists who wish to consider new ideas in a novel laboratory environment and to engineers concerned with advanced technologies of materials processing.

594 pp., 6x9, illus., \$20.00 Member \$35.00 List

TO ORDER WRITE: Publications Dept., AIAA, 1290 Avenue of the Americas, New York, N.Y. 10019